XV. Space Instruments

SPACE SCIENCES DIVISION

A. Range of Applicability for the Photometric Method of Topographic Mapping, *T. Rindfleisch*

1. Summary

In Ref. 1 a method is discussed for extracting topographic information about the Moon for monoscopic photographs using a knowledge of the lunar photometric properties (Ref. 2). This method is attractive for space applications since it does not require the redundant photographic coverage used in stereoscopy, but requires instead a detailed knowledge of the surface photometric properties. In applying the method to the lunar surface, it was necessary to use certain symmetry properties of the lunar photometric function to integrate the general differential equation. The purpose of this note is to examine the applicability of the method to surfaces with photometric properties different from those of the Moon. The conclusion will be that only a slight generalization in photometric function symmetries from those of the Moon is possible while still being able to integrate the basic equation.

2. Discussion

Representing points on an object surface by position vectors with respect to the center of the camera lens, it can be shown (Ref. 1) that the directional derivative of the length of the vector to a point with respect to distance in the image plane is given by

$$\frac{d}{dS}(\ln r) = \frac{1}{F}\frac{(\hat{\mathbf{r}}\cdot\hat{\mathbf{z}})}{(\hat{\mathbf{N}}\cdot\hat{\mathbf{r}})}[\hat{\mathbf{r}}\times(\hat{\mathbf{N}}\times\hat{\mathbf{r}})]\cdot\hat{\mathbf{S}}_T \qquad (1)$$

The symbols in Eq. (1) are defined (see Fig. 1) as

- $\mathbf{r}$ = the position vector to an object point (to be determined)
- r = the length of $\mathbf{r}$ (to be determined)
- $\hat{\mathbf{r}}$ = a unit vector along $-\mathbf{r}$; $\hat{\mathbf{r}} = -\mathbf{r}/r$ (known from image geometry)
- F = the focal length of the camera lens (known)
- $\hat{\mathbf{z}}$ = a unit vector along the optical axis (known)
- $\hat{\mathbf{S}}_T$ = a unit vector in the image plane along the direction of differentiation (arbitrary)
- S = a distance variable in the image plane (along $\hat{\mathbf{S}}_T$)
- $\hat{\mathbf{N}}$ = a local unit normal to the object surface (unknown except through the surface photometric properties and the recorded picture brightness)

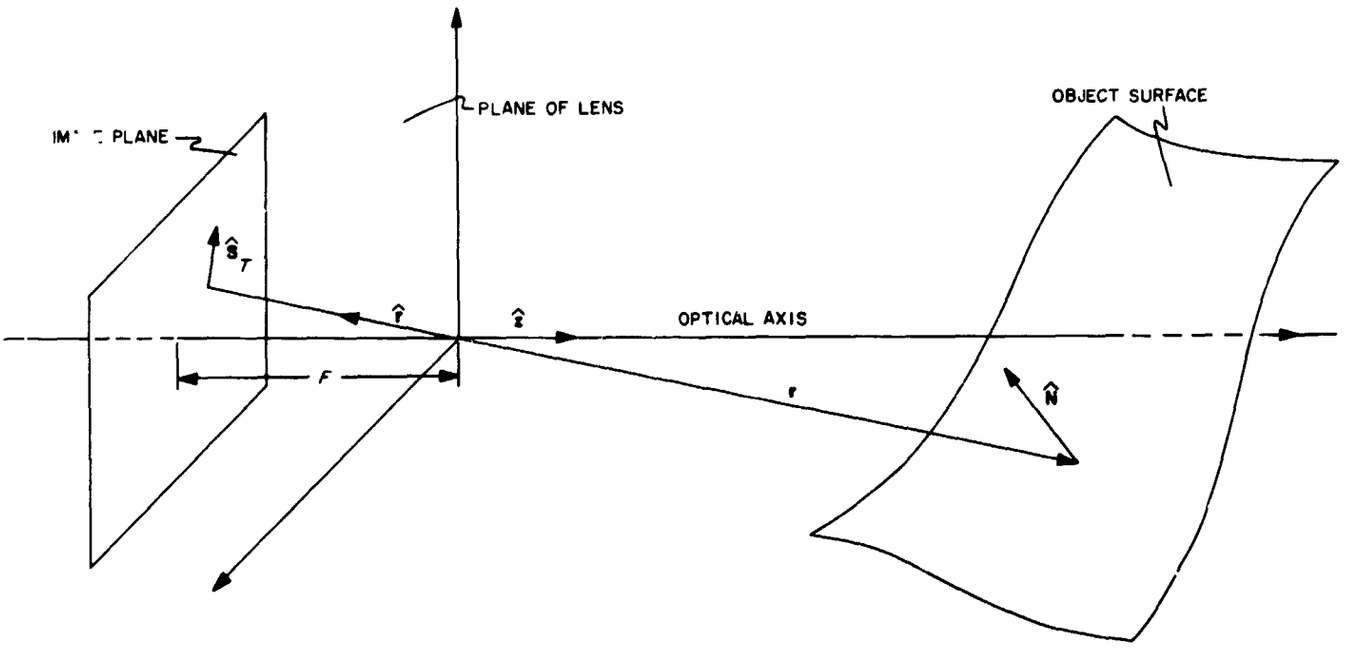

Fig. 1. Definition of image geometry

If the direction $\hat{\mathbf{N}}$ were known, the right side of Eq. (1) could be evaluated for any direction $\hat{\mathbf{S}}_T$ in the image plane. However, the only information about $\hat{\mathbf{N}}$ that is actually available comes through the surface photometric function

$$b = b(\hat{\mathbf{N}}, \hat{\mathbf{r}}, \hat{\mathbf{R}}) \tag{2}$$

which expresses the apparent brightness b as a function of the *relative* orientations of the surface normal direction $\hat{\mathbf{N}}$, the viewing direction $\hat{\mathbf{r}}$, and the illumination direction $\hat{\mathbf{R}}$ (it is assumed the illumination is uniform, collimated, and from a known direction).

Since it takes two angles to specify the direction $\hat{\mathbf{N}}$, Eq. (2) and a given observed surface brightness b are insufficient to completely determine $\hat{\mathbf{N}}$. Thus the right side of Eq. (1) cannot be evaluated for an arbitrary differentiation direction $\hat{\mathbf{S}}_T$ using *only* photometric information. The problem is to determine the conditions under which a direction $\hat{\mathbf{S}}_T$ can be found so that Eq. (2) can be used to integrate Eq. (1). (Ref. 1 discusses the solution for the lunar case.)

It is convenient to describe the photometric geometry in terms of the angles α, β, and g used in Ref. 1 and shown in Fig. 2.

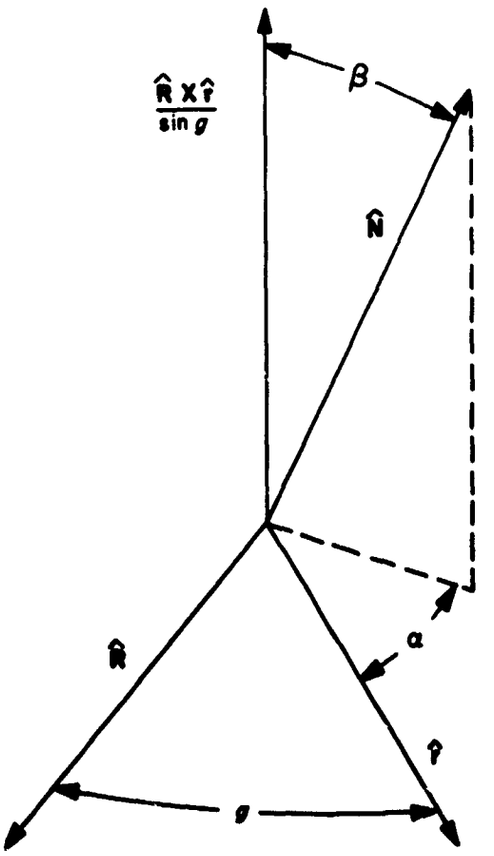

Fig. 2. Definition of photometric angles

Using these angles, Eqs. (1) and (2) become

$$\frac{d}{dS}(\ln r) = \frac{1}{F}(\hat{\mathbf{r}}\cdot\hat{\mathbf{z}})\left\{\frac{\cot\beta}{\cos\alpha}\left(\frac{\hat{\mathbf{R}}\times\hat{\mathbf{r}}}{\sin g}\right) - \tan\alpha \times\left[\hat{\mathbf{r}}\times\left(\frac{\hat{\mathbf{R}}\times\hat{\mathbf{r}}}{\sin g}\right)\right]\right\}\cdot\hat{\mathbf{S}}_T \tag{1a}$$

and

$$b = b(\alpha, \beta, g) \tag{2a}$$

It is also convenient to decompose the vector $\hat{\mathbf{S}}_T$ along a coordinate system with basis vectors $\hat{\mathbf{r}}$, $(\hat{\mathbf{R}}\times\hat{\mathbf{r}})/\sin g$, and $[\hat{\mathbf{r}}\times(\hat{\mathbf{R}}\times\hat{\mathbf{r}})]/\sin g$ as shown in Fig. 3. Letting δ be a measure of the direction of $\hat{\mathbf{S}}_T$ (i.e., the angle between the component of $\hat{\mathbf{S}}_T$ perpendicular to $\hat{\mathbf{r}}$ and the basis vector $[\hat{\mathbf{r}}\times(\hat{\mathbf{R}}\times\hat{\mathbf{r}})]/\sin g$), one can write

$$\hat{\mathbf{S}}_T = (\hat{\mathbf{S}}_T\cdot\hat{\mathbf{r}})\,\hat{\mathbf{r}} + \sqrt{1-(\hat{\mathbf{S}}_T\cdot\hat{\mathbf{r}})^2}\left[\sin\delta\left(\frac{\hat{\mathbf{R}}\times\hat{\mathbf{r}}}{\sin g}\right) + \cos\delta\left(\frac{\hat{\mathbf{r}}\times(\hat{\mathbf{R}}\times\hat{\mathbf{r}})}{\sin g}\right)\right] \tag{3}$$

where

$$\hat{\mathbf{S}}_T\cdot\hat{\mathbf{r}} = \frac{\hat{\mathbf{z}}\cdot\left[\sin\delta\left(\frac{\hat{\mathbf{R}}\times\hat{\mathbf{r}}}{\sin g}\right) + \cos\delta\left(\frac{\hat{\mathbf{r}}\times(\hat{\mathbf{R}}\times\hat{\mathbf{r}})}{\sin g}\right)\right]}{\left\{(\hat{\mathbf{r}}\cdot\hat{\mathbf{z}})^2 + \left[\sin\delta\,\frac{\hat{\mathbf{z}}\cdot(\hat{\mathbf{R}}\times\hat{\mathbf{r}})}{\sin g} + \cos\delta\,\frac{\hat{\mathbf{z}}\cdot[\hat{\mathbf{r}}\times(\hat{\mathbf{R}}\times\hat{\mathbf{r}})]}{\sin g}\right]\right\}^{1/2}}$$

Substitution of Eq. (3) into Eq. (1a) yields

$$\frac{d}{dS}(\ln r) = \frac{1}{F}(\hat{\mathbf{r}}\cdot\hat{\mathbf{z}})\sqrt{1-(\hat{\mathbf{S}}_T\cdot\hat{\mathbf{r}})^2}\left[\frac{\cot\beta}{\cos\alpha}\sin\delta - \tan\alpha\cos\delta\right] \tag{4}$$

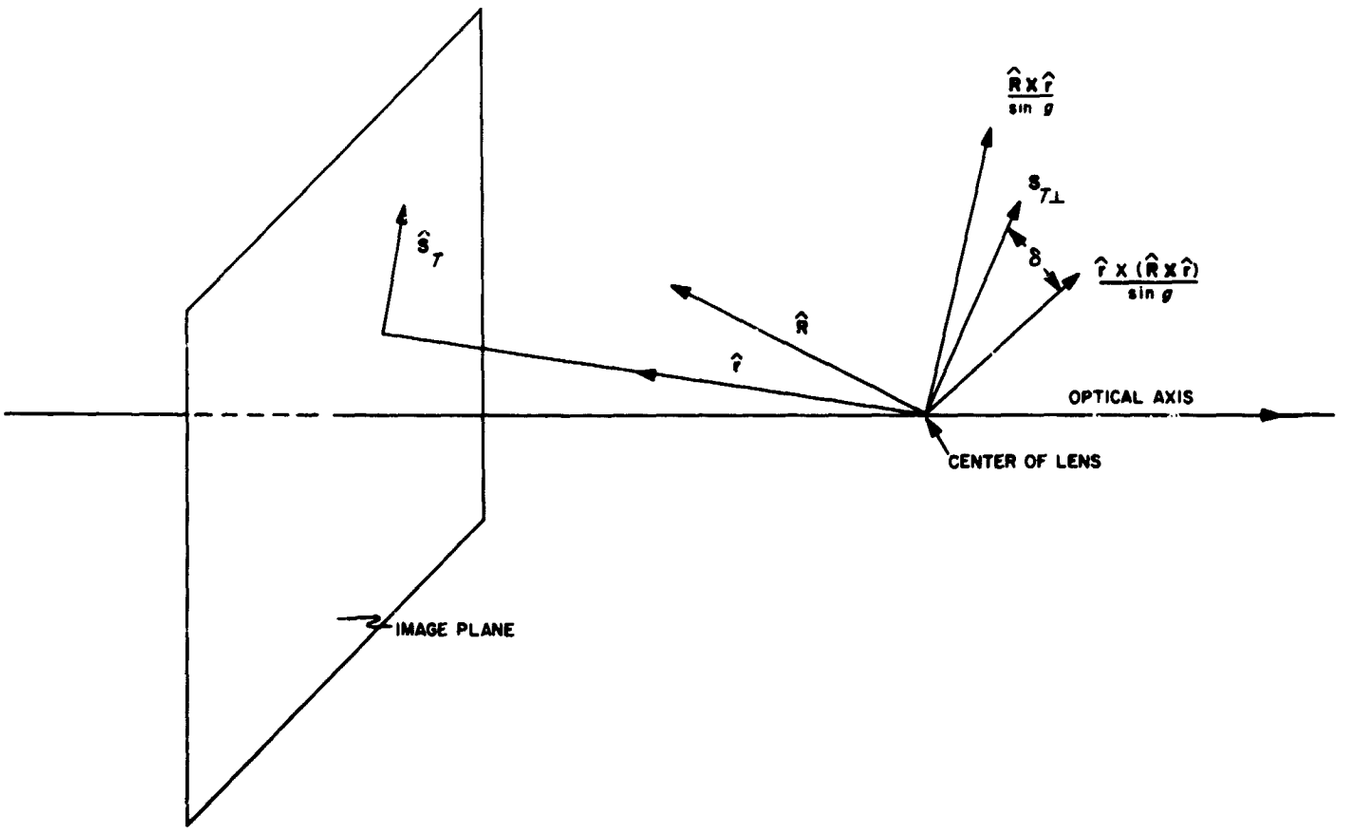

Fig. 3. Coordinate decomposition of $\hat{\mathbf{S}}_T$

Since the topography is independent of the camera orientation, in order to integrate Eq. (4), both the angle δ and the quantity ϕ, where

$$\phi = \frac{\cot \beta}{\cos \alpha} \sin \delta - \tan \alpha \cos \delta$$

must be derivable from the known phase angle g and the measured brightness b related through Eq. (2a). Thus, to proceed with the integration, there must exist relations of the form

$$\phi = \phi(b, g)$$

and

$$\delta = \delta(b, g)$$

which can, in principle, be inverted to give

$$\left.\begin{aligned} b &= b(\phi, g) \\ \delta &= \delta(\phi, g) \end{aligned}\right\} \tag{5}$$

Thus, for constants b and g, ϕ and δ must be constant so that isophotes are given by

$$\frac{\cot \beta}{\cos \alpha} \sin \delta - \tan \alpha \cos \delta = \text{constant} \tag{6}$$

and

$$g, \delta = \text{constants}$$

Eq. (6) determines the locus of α and β for which the hypothetical surface must exhibit constant brightness. It is straightforward geometry to show that in a coordinate system rotated an angle δ opposite to a right-hand screw about the axis $\hat{\mathbf{r}}$ of Fig. 2, Eq. (6) takes on the simple form

$$\tan \alpha' = \text{constant} \tag{6a}$$

where the angle α' is the azimuth of $\hat{\mathbf{N}}$ in the rotated system (see Fig. 4).

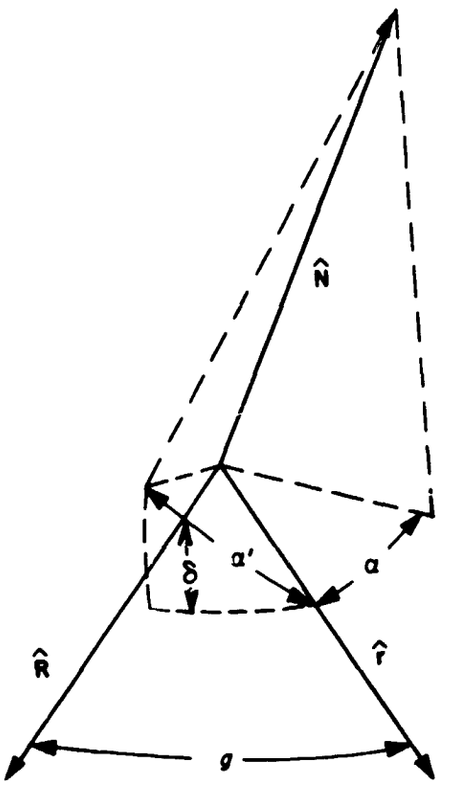

Fig. 4. Rotated photometric geometry

It will be noted that this situation is a generalization of the lunar case for which $\delta \equiv 0$, $\phi \equiv -\tan \alpha$, and, as observed experimentally (Ref. 2),

$$b = b(\alpha, g)$$

The physical consequences of a case different from the Moon ($\delta = 0$) are most easily visualized by considering the topology of isophotes on a sphere having the hypothetical photometric properties (see Fig. 5). For given illumination and viewing directions and assuming $\delta \neq 0$, isophotes will be great circles inclined to the plane containing g and *intersecting* the terminator (note that for $\delta = 0$, the isophotes run parallel to the terminator in a spherical sense; i.e., the isophotes are a family of great circles with a common diameter). The isophotes must also be symmetric above and below the plane of g, as is clear from the previous discussion.

Certainly, Lambertian-like matt surfaces do not exhibit such properties. Whether or not surfaces of bodies of the solar system other than the Moon exhibit this type of symmetry is an open question, since little detailed photometric information is available because of poor resolution, angular variation, and atmospheres.

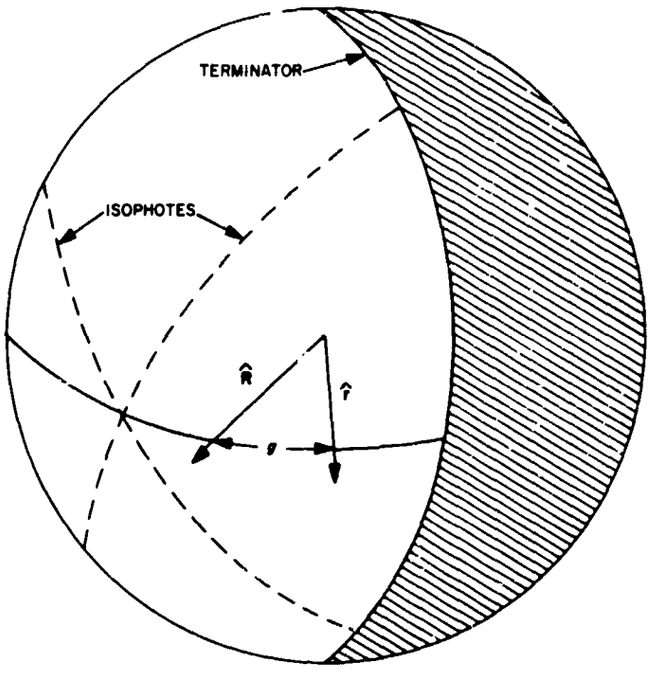

Fig. 5. Isophotes on a sphere with generalized photometric properties

3. Conclusion

It has been shown that the geometrical equation derived in Ref. 1 can be integrated photometrically only for a class of surfaces having reflectance properties that are a simple generalization of those of the Moon. Clearly excluded from this class are Lambertian-type matt surfaces typified by finely divided materials. It is not well known if lunar photometric properties are common to other soils of the solar system. Earth-type soils do not exhibit photometric properties similar to those of the Moon, indicating that erosion processes may be important. In any case, the applicability of the photometric method for topographic mapping appears to be severely limited.

B. Residual Signal and Image Storage of Several Slow-Scan Vidicons, *L. R. Baker*

1. Introduction

As a part of the photosensor evaluation supporting research program,[1] a series of tests were performed on various slow-scan vidicons. The purpose of these tests was to obtain a better understanding of the physical problems of vidicon operation at slow scanning rates.

[1]NASA Work Unit 125-24-01-03.

Ever since television systems have been required to operate at data rates lower than standard television rates (525 line, 60 fields/sec), problems have arisen with the image sensor. The very low data transmission rate from planetary spacecraft places very special requirements on image sensors to be used in scientific instruments. In particular, residual signal (erase) and image storage are very important image quality characteristics of a slow-scan vidicon. Residual signal, which refers to the signal remaining after one *expose-read* cycle, is important since residual signal from a previous exposure will appear in the picture as coherent noise and decreases the signal-to-noise ratio. Image storage, which refers to the signal remaining after a long period of time between exposure and readout, is important since the vidicon signal output at the bottom of the frame should be equal to the signal at the top of the frame (excluding beam landing errors and optical vignetting effects). Additionally, the preservation of fine detail for long periods is associated with image storage.

2. Test Procedure

The following procedure was used to evaluate image storage and erase of nine slow-scan vidicons. The procedure was designed to determine long-term image storage capability and the ability of the photoconductor to recharge to cathode potential so as to erase the previously exposed image.

The vidicon was operated in a 950-line, 8.33-msec/line slow-scan mode using a calibrated shutter of 60-msec exposure time. The video bandwidth was set at 100 kHz.

a. Residual signal tests. A high-contrast, small area, black bar pattern was imaged on the vidicon target, using a calibrated slide illuminator and a calibrated 50-mm lens. The faceplate illumination was calculated to be 0.076-ft-c sec at f/5.6. The photoconductor was allowed to completely recharge; then one single exposure was taken. Single-line photographs of the center of the raster were taken of the initial, second, third, and fourth readouts. The ratio of signal remaining to initial signal was measured from the photographs.

b. Image storage tests. The same test pattern was used as in the residual signal test, and the faceplate illumination was 0.076-ft-c sec. The photoconductor was allowed to completely recharge; then the beam current was cut off by applying −140 v to the vidicon control grid, and a single exposure was taken. After waiting a predetermined length of time, the control grid bias was set to normal.

Table 1. Test results

Vidicon serial No.	Use	Photoconductor	Residual, %			Image storage, %				Vidicon manufacturer	Vidicon type
			2nd read	3rd read	4th read	30	60	90	120		
Z07731	Experimental sterilizable	Modified ASOS	35	23	16	42	35	32	26	RCA	7735a
Z12227	Experimental sterilizable	Modified ASOS	75	53	30	70	47	43	23	RCA	7735a
2125858	*Rangers VI–IX*	ASOS	31	15	10	21	0	0	0	RCA	C74072
9-23-271	General slow-scan	Se	16	0	0	100	92	88	87	West	WL7290
3-6-675	Experimental *Ranger*	Se	13	0	0	100	64	51	41	West	WX4783
2538436	General slow-scan	Modified Se	19	0	0	63	44	34	32	GEC	TD1368
2538450	General slow-scan	Modified Se	34	13	8	100	92	83	80	GEC	TD1368
0473122	*Mariner Mars* 1969	Modified Se	23	9.6	0	100	100	89	89	GEC	TD1342-011
0473132	*Mariner Mars* 1969	Modified Se	39	12.2	9.7	98	102	98	90	GEC	TD1342-011

A photograph of a single line of video was taken from the center of the raster. The signal amplitude at the end of the image storage period was compared to the non-stored signal amplitude. The storage times used were 30, 60, 90 and 120 sec. The results of these tests are given in Table 1.

3. Summary and Conclusions

A number of conclusions can be drawn from the test results. The physical operation of antimony-sulfide-oxide-sulfide (ASOS) and selenium-based photoconductors is substantially different. ASOS is a modification of the standard Sb_2S_3 photoconductor and operates as a very "laggy" vidicon; it does not exhibit true charge storage. The selenium-based photoconductors generally show a lower residual signal and better image storage, indicating an operation closer to true charge storage. The effect is probably due to higher resistivity and fewer electron traps in selenium-based photoconductors. The percentage of signal removed during each scan is shown in Table 2. These data show that ASOS photoconductors have less signal removed per scan than the other photoconductors, verifying the "lag" and "stickiness" of ASOS. In other words, ASOS not only has a higher residual signal, but retains the residual signal for a longer period of time.

Table 2. Signal removal via scanning

Vidicon serial No.	Residual signal removal, %		
	2nd to 3rd read	3rd to 4th read	2nd to 4th read
Z07731	34	31	54
Z12227	27	43	59
2125858	52	33	68
9-23-271	100	—	—
3-6-675	100	—	—
2538436	100	—	—
2538450	62	38	77
0473122	58	100	—
0473132	69	21	75

The tests discussed in this report were carried out on a small sample of vidicons and are not entirely conclusive. However, additional tests are not expected to show any change in the existing trends. The low storage and high residual image characteristics of ASOS are parameters that have caused and will continue to cause great difficulties in the design of future television instruments.

It should be noted that although selenium has very attractive image quality characteristics, it has an absolute upper temperature limitation of 45°C. This is too low for planetary spacecraft, where temperature control is a problem. Modified selenium will go to 55°C and has good image characteristics, and is therefore a photoconductor that finds acceptance and application to interplanetary photography

References

1. Rindfleisch, T., "Photometric Method for Lunar Topography," *Photogrammetric Engineering*, Vol. 32, No. 2, pp. 262–276, March 1966.
2. Willingham, D. E., *The Lunar Reflectivity Model for Ranger Block III Analysis*, Technical Report 32-664, Jet Propulsion Laboratory, Pasadena, Calif., November 2, 1964.